General Disclaimer

One or more of the Following Statements may affect this Document

- This document has been reproduced from the best copy furnished by the organizational source. It is being released in the interest of making available as much information as possible.

- This document may contain data, which exceeds the sheet parameters. It was furnished in this condition by the organizational source and is the best copy available.

- This document may contain tone-on-tone or color graphs, charts and/or pictures, which have been reproduced in black and white.

- This document is paginated as submitted by the original source.

- Portions of this document are not fully legible due to the historical nature of some of the material. However, it is the best reproduction available from the original submission.

Produced by the NASA Center for Aerospace Information (CASI)

ABSTRACT

Specimens of gas saturated carbon tetrabromide were directionally solidified in a transparent furnace using a gradient freeze technique. The original temperature gradient as 5°C/cm and the cooling rate was 40°C/h. Progress of the experiment was monitored hotographically. Gas bubbles were generated at the advancing solidification front in each f the three specimens (argon, hydrogen, and nitrogen saturated, respectively). The as bubbles were observed to increase in size, coalesce, and eventually be grown into the olid specimen under low-gravity conditions. No bubble detachment from the interface was bserved. Identical specimens processed in the laboratory showed bubble nucleation, ubble growth, and eventual bubble detachment due to buoyancy forces. Examination of he specimens showed a significantly greater void content in the low-gravity processed amples. The grain size was observed to be finer in the low-gravity processed samples. ubbles, 50 μm to 4 mm in diameter, situated in the melt well ahead of the interface did ot migrate to the hot end of the sample tube; this is contrary to predictions of thermal nigration of bubbles in the absence of gravity. Reasons for this observation are discussed.

Grumman Research Department Memorandum RM -616

FLIGHT I TECHNICAL REPORT FOR
EXPERIMENT 74-36

THERMAL MIGRATION OF BUBBLES AND
THEIR INTERACTION WITH SOLIDIFICATION INTERFACES**

by

John M. Papazian†

and

William R. Wilcox††

† Research Department, Materials and Structural Mechanics
†† Department of Chemical Engineering
   Clarkson College of Technology
   Potsdam, N.Y. 13676

April 1976

Approved by: *Charles E. Mack Jr.*
Charles E. Mack Jr.
Director of Research

RM-616

FLIGHT I TECHNICAL REPORT FOR
EXPERIMENT 74-36

THERMAL MIGRATION OF BUBBLES
AND THEIR INTERACTION WITH
SOLIDIFICATION INTERFACES

April 1976

RESEARCH DEPARTMENT

GRUMMAN AEROSPACE CORPORATION
BETHPAGE NEW YORK

TABLE OF CONTENTS

LIST OF ILLUSTRATIONS

I. INTRODUCTION

This report presents the results obtained from experiment 74-36 on the SPAR I sounding rocket flight. The primary objective of this experiment is to observe directly the interaction of solidification interfaces with bubbles in the absence of gravitational forces. In addition, we hope to generate some preliminary information on the rate of migration of bubbles in a quiescent liquid in a temperature gradient. These phenomena are of interest because bubbles are more of a problem in a gravity-free materials processing due to the lack of buoyancy, the decreased hydrostatic head, decreased free convection, and increased dispersion of foreign particles. These factors lead to easier nucleation and slower motion of bubbles in microgravity. The understanding and control of bubble dynamics and bubble-interface interactions will be important elements in the development of sound materials processing practices in the orbital environment. Further, the microgravity environment allows us to perform experiments which are impossible on earth but nevertheless produce results pertinent to problems encountered in earth-based material processing.

The usual difficulties encountered in performing an experiment are exacerbated by the unique characteristics of a sounding rocket flight. The 300s microgravity interval is preceeded by violent accelerations due to engine thrust, spin stabilization, de-spin and a complex vibrational spectrum. Thus, the apparatus must be robust and the experimental configuration must be designed to minimize the effects of the launch environment. In addition, a rapidly changing vacuum and thermal profile is imposed upon the apparatus by the rocket trajectory. Naturally, all manipulations must be performed by remote control. In light of these constraints the philosophy adopted in this experiment was one of simplicity, redundancy, and low power requirements.

The philosophy led naturally to the choice of low melting point, transparent, organic materials to simulate the solidification behavior of metals. Prior experiments have clearly established the utility and applicability of this technique (Ref. 1). Besides their attractive low melting points, these materials possess the unique advantage of being transparent. Thus the progress of the experiment can be monitored photographically to produce a record of the sequence of events. This adds an extra dimension of insight into the physical processes and is a decided advantage over simply trying to reconstruct the sequence of events through specimen analysis.

Unstated, but very important, additional objectives of the first flight were to evaluate the effects of launch induced fluid motion on a partially liquid-partially solid specimen, to gauge the time required for damping of such fluid motion, and to gain a better understanding of the thermal and barometric environment seen by the apparatus during the rocket flight.

1

II. EXPERIMENTAL PROCEDURE

A. Apparatus

In its simplest form the apparatus for this experiment was required to perform the following functions:

- Establish a predetermined temperature gradient along the length of three specimens

- Freeze the specimens at a predetermined rate during the microgravity interval of the flight

- Photographically record the progress of the solidification front and the motion of any bubbles

- Provide a record of the thermal history of the specimen.

Such an apparatus was designed, built, qualification tested and then successfully flown on SPAR I. An overall view of the apparatus is shown in Fig. 1. The apparatus consists of four basic units. The first is the frame, which serves to physically support the three working components and attaches directly to the mounting tabs of the Black Brant rocket. The second component is an electronics package, which contains an analogue timer-sequencer controlling the operation of the camera and lights, a power supply for the camera and lights and a 15-channel signal conditioner to convert the thermistor outputs to a 0-5 VDC signal suitable for the rocket's telemetry system. The electronics package was powered by the main on-board 28V rocket battery and started by the lift-off switch. The third component was the GFE motorized 250 exposure 35mm Nikon F2 camera which was contained in a supporting box. The camera used a Nikon 55mm MICRO lens set to photograph at 1/2X magnification. The fourth component was the specimen holder/furnace assembly. This consisted of an aluminum block which accommodated the four 10 x 100mm sample tubes, housed the lighting system, and contained the heaters. The heaters were located at the top and bottom of the block and were powered by 110 VAC through the unbilical cable. The temperatures of the top and bottom portions of the specimen holder are preset and controlled independently by two temperature controllers housed in the ground support equipment electronic package. Specimen temperature measurements were made by an array of fourteen thermistors which were bonded to the back of the specimen holder.

In operation, the heaters were activated 30 to 45 minutes before launch and thereby a stable temperature gradient was established and maintained along the length of the specimen holder. Upon launch the umbilical connection was ruptured and the specimen holder began to cool at a rate determined by the ambient temperature and pressure and by the thermal
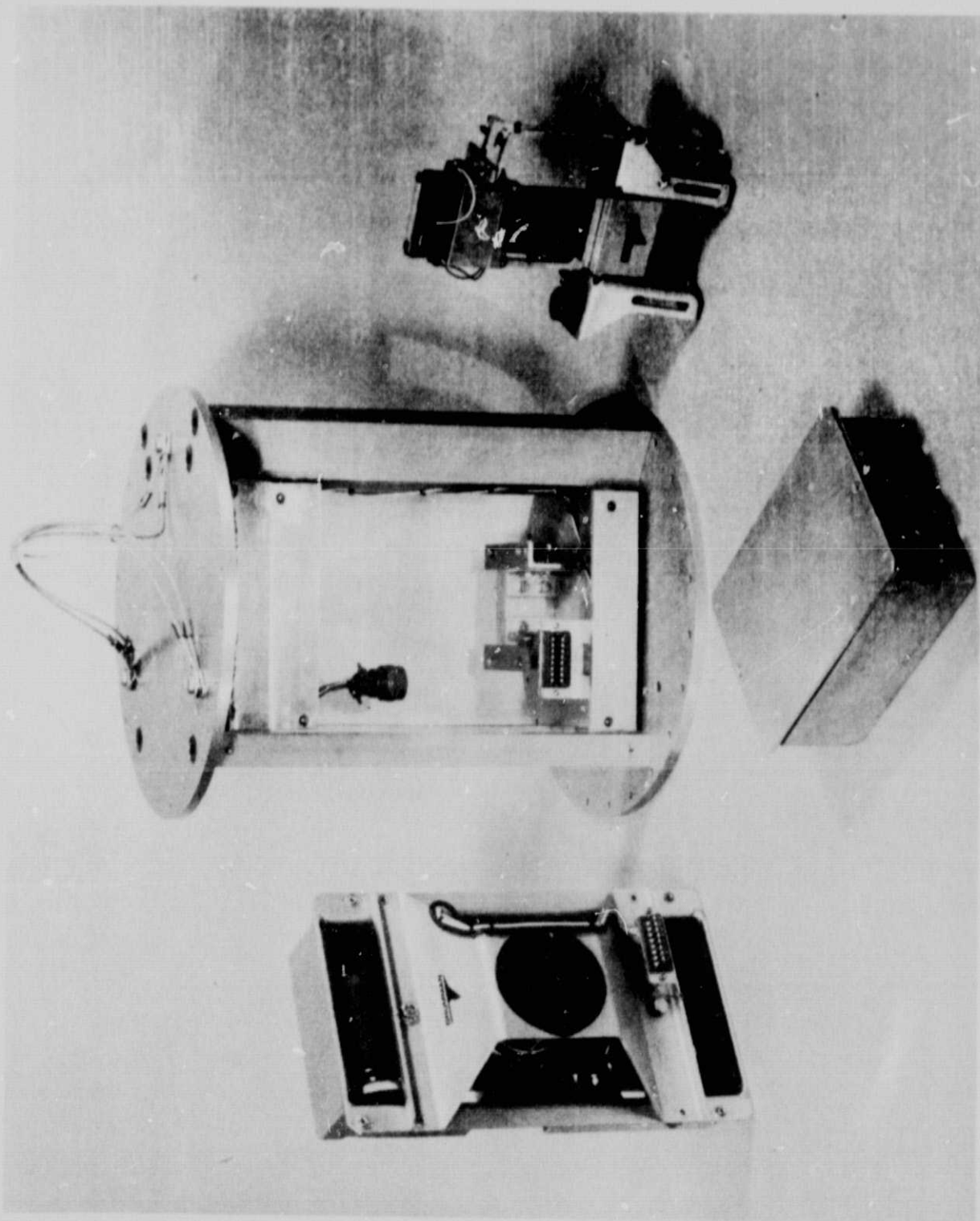
2

Figure 1 Gradient freeze apparatus built for experiment 74-36, SPAR I

3

conductivity of the specimen holder mounts. This was adjusted in the laboratory to provide approximately the desired solidification rate of 10 μm/s. The block temperatures recorded during a ground base simulation (GBS) are shown in Fig. 2. This GBS was performed by turning off heater power and rough pumping the bell jar in which the apparatus was installed at time zero. The actual cooling rate during flight 1 is shown in Fig. 3. It is seen that cooling was slower during the rocket flight. Since no change was detected in the temperature of the base plate during the flight we conclude that atmospheric conduction losses were lower during the flight and thus we must pump out the system more quickly to perform an accurate GBS.

B. Specimen Preparation

Carbon tetrabromide was chosen as the sample material for this investigation. The choice was made on the basis of previously published results, melting point (90°C), and availability. The material was from lot no. A4C of Eastman Chemicals. The samples were contained in 10 x 100mm pyrex tubes which were sealed at one end by a glassblower. The seal at the other end was effected by a nylon stopper having two "O" rings. The stopper was at the bottom (cold) end of the tube. Numerous GBS tests were performed to establish conditions of sample preparation which would ensure reliable and copious evolution of bubbles during the experiment. The preparation sequence finally chosen was as follows:

- Melting of as-received crystalline CBr_4 in the sample tube in a thermostatically controlled 95°C furnace

- Bubbling of A, H_2 or N_2 through the molten CBr_4 for five minutes

- Stopper insertion and rapid cooling.

All of these manipulations were carried out in an argon-filled dry box which was shielded from short wavelength light by filters. It had previously been determined that liquid CBr_4 decomposes rapidly in the presence of light. Numerous reactions are possible; in most cases, highly reactive bromine radicals and free bromine are produced. These reaction products caused rapid discoloration of the specimen and vigorously attacked the stopper and "O" rings. In order to suppress this photolysis, filters were installed on the specimen holder and dry box such that no light with a wavelength of less than 420nm could reach the specimen. In addition, dwell time in the liquid state was kept to a minimum. The gas filled volume in the sample tube (ullage) was adjusted to be approximately zero when the sample was half molten – half solid, the anticipated launch configuration.

4

THERMAL PROFILE. SPEC 2. 18AUG75

TEMPERATURE. DEGREES C

SPECIMEN LENGTH. CENTIMETERS

t=0
t=50s
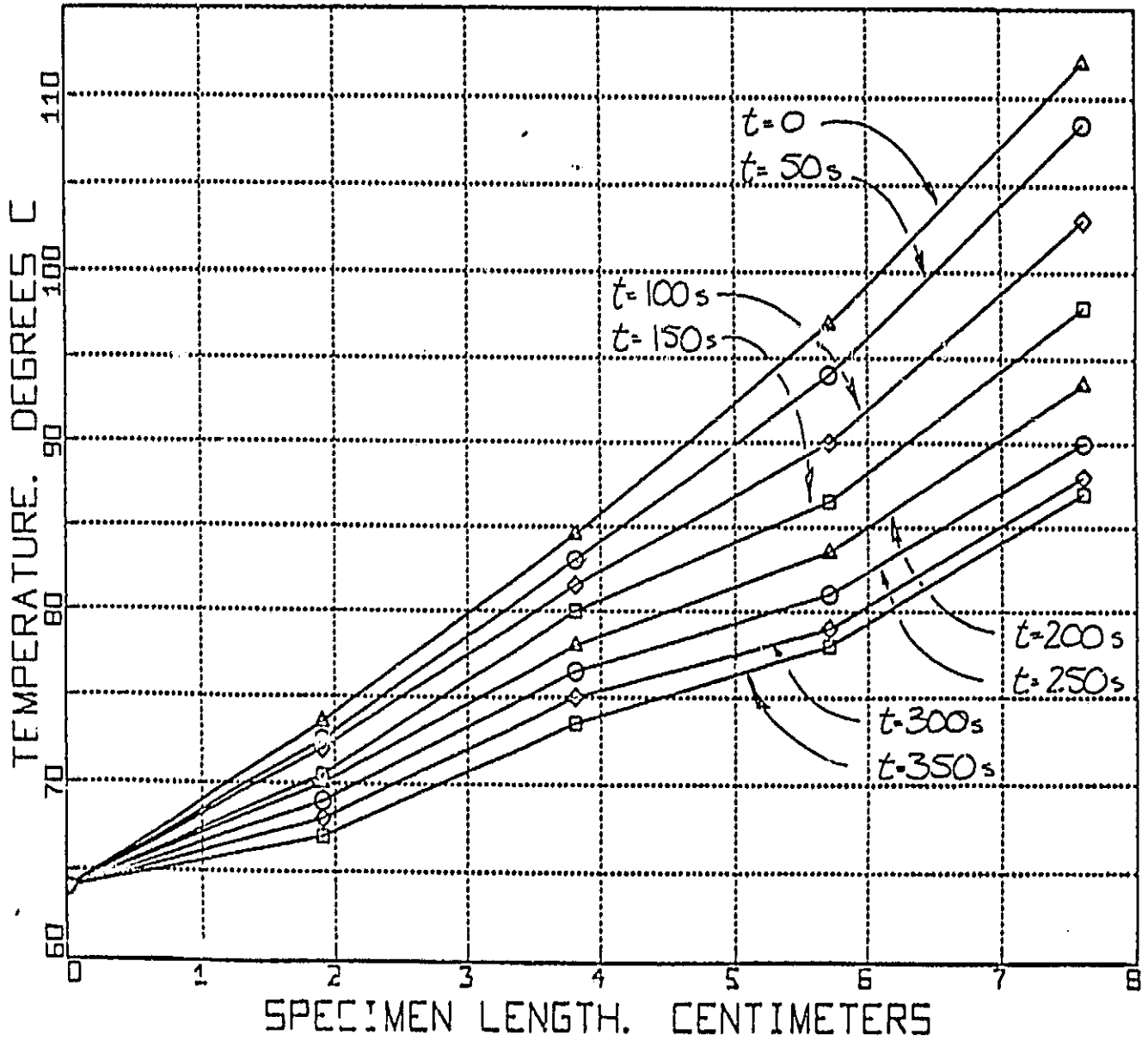t=100s
t=150s
t=200s
t=250s
t=300s
t=350s

Figure 2 Thermal history of furnace block, GBS, 18 Aug 1975

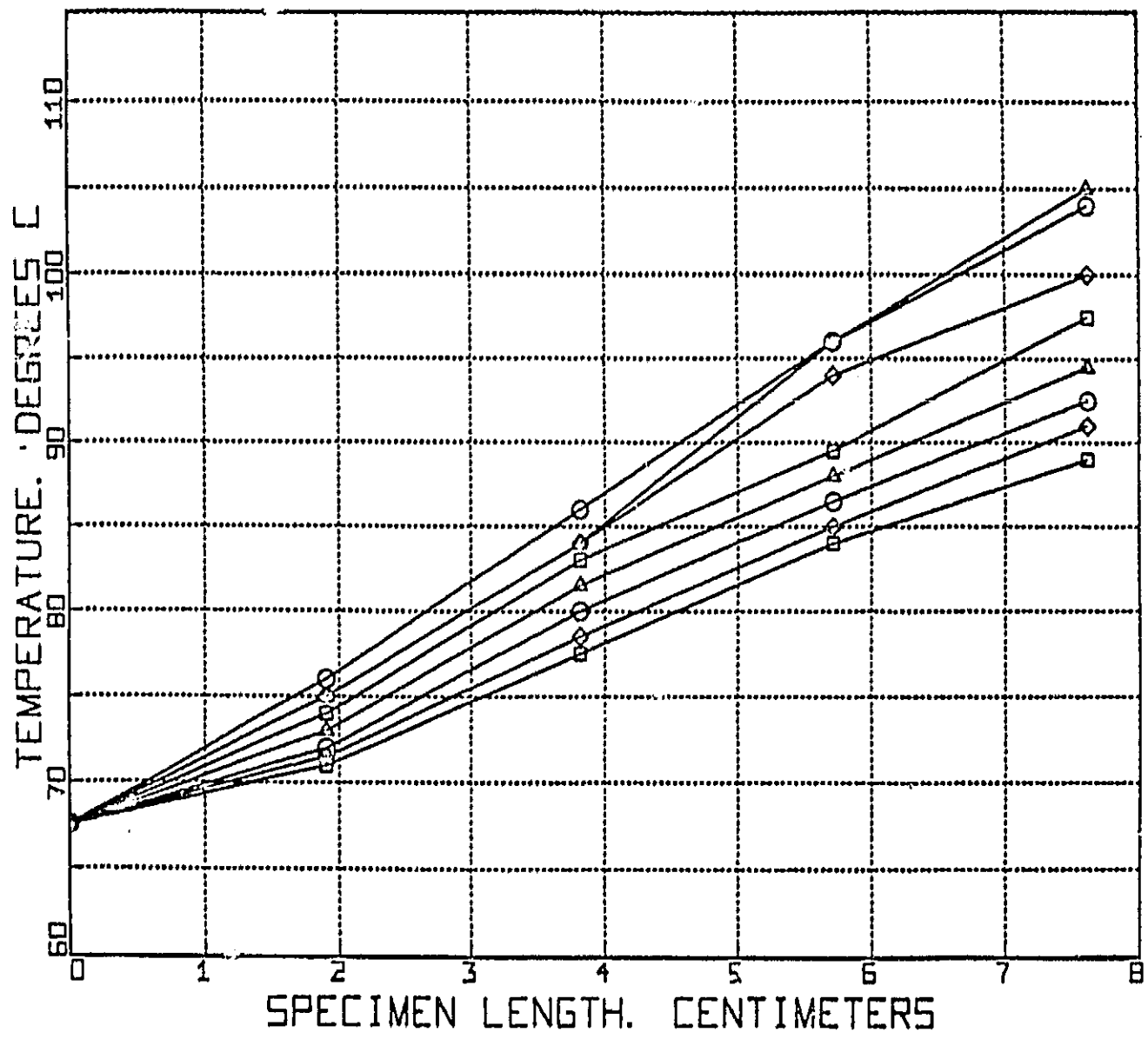# THERMAL PROFILE. SPEC 2 FLIGHT 11DEC75

Figure 3 Thermal history of furnace block, Flight, 11 Dec 1975

6

III. RESULTS

A. Initial Observations

During the actual rocket flight the apparatus functioned perfectly and the experiment was performed according to plan.

The major results of this experiment are contained in the 220 exposure 35mm film which was taken during flight. The camera began framing at 80s after lift off and recorded at the rate of approximately one frame per second. This time lapse sequence of pictures has been made into a 16mm film*. Each original image was repeated eight times on the 16mm film in order to partially adjust the one frame per second filming rate to normal projection rate (24 fps). Thus, when viewing the film, the actual experiment is speeded up by a factor of three. Initial observations of the film show significant generation, motion, and inclusion of bubbles in the mushy zone, the disappearance of small bubbles in the liquid, and little, if any, motion of bubbles in the quiescent liquid. In addition to the film record, other data were generated by analysis of the returned specimens. Results from these two sources of information are discussed below.

B. Photographic Observations

Three frames from the 220 exposure flight sequence are reproduced in Figs. 4, 5 and 6. These photos cannot adequately portray the dynamics of the experiment but they are intended to show a rough outline of the results. Figure 4 shows the appearance of the samples at t=85s. The extreme left hand tube, specimen A, is from experiment 74-15 of MIT and contains naphthalene to which various small particles had been added. The next tube, specimen B, was argon saturated CBr_4; specimen C was hydrogen saturated CBr_4 and specimen D was nitrogen saturated CBr_4. All of the specimens were situated in the thermal gradient shown in Fig. 3. The bottoms of the specimens were at the cool end and thus the lower portions of all the specimens were solid. (Naphthalene melts at 80°C and carbon tetrabromide melts at 90°C.)

Specimen A shows a vortex-like structure in the liquid just ahead of the interface. This feature is interpreted as being the image of small particles that were resting on the liquid-solid interface before launch and which were swept up by fluid motion during rocket spin and de-spin. The shape of this feature does not change during the 220s series of photographs. This observation leads to these conclusions: (1) that significant fluid motion

* One copy of this film has been submitted to the SPAR program office at MSFC. A loan copy is available to interested parties from the authors.

7

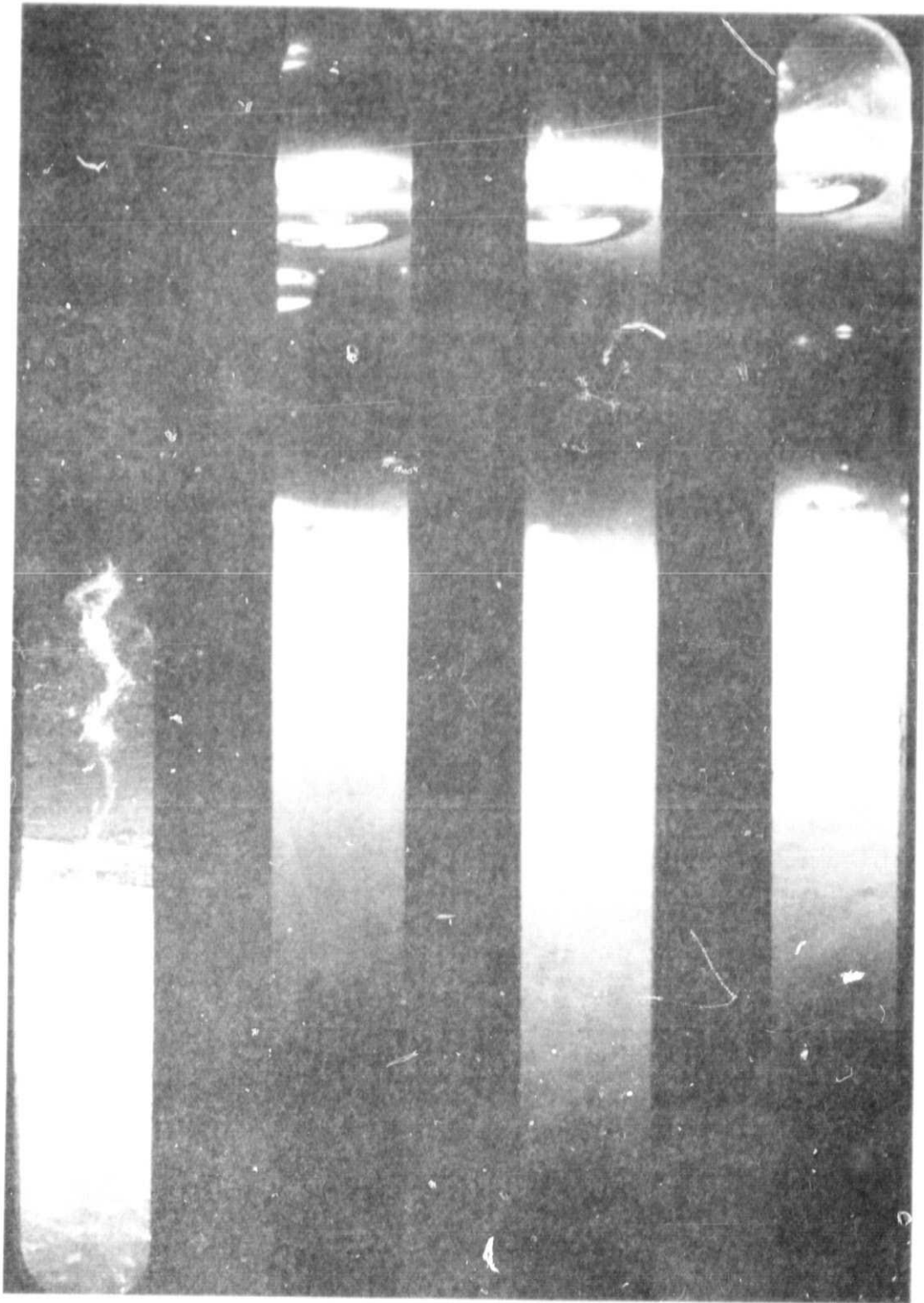Figure 4 Photograph of experiment at t = 88s after lift off

8

Figure 5 Photograph of experiment at t = 155s

9

Figure 6 Photograph of experiment at t = 305s

10

occurred during launch, (2) that the fluid motion was predominately axial rather than longitudinal and (3) that fluid motion had been damped out by t=80s. The viscosity of naphthalene varies from 0.97 at 80°C to 0.78 at 100°C (Ref. 2) and microgravity was not completely established until approximately t=75s. Thus the damping occurred very rapidly, even more rapidly than had been expected (Ref. 3). Comparison with photographs taken immediately before launch shows that the fluid motion during launch caused approximately 1 to 2mm of melting back or erosion of the solid-liquid interface in the CBr_4 specimens.

Specimens B, C, and D contained bubbles in the liquid portion of the sample tubes. The images of the bubbles were all distorted by the cylindrical sample tubes. Control experiments in which transparent plastic spheres were photographed at different positions in the sample tube showed that a spherical object is distorted such that the vertical dimension (along the length of the tube) is unchanged but the horizontal dimension is greatly magnified. Thus, the bubbles were in fact spherical and had a diameter equal to their apparent height.

Large bubbles of approximately 4mm diameter are present in all three tubes and smaller bubbles, down to 40 μm diameter, were present in tubes B and D. The bubbles were generated during the launch phase of the flight and were probably dispersed through the liquid by buoyancy and launch-induced fluid motion. The bubbles could have been due to evolution of trapped gas during melt back, nucleation and growth of bubbles of gaseous solute rejected during solidification, or dispersal of gas present before launch. They probably are due to a combination of the three mechanisms. It seems likely that the 4mm bubbles near the top of each tube were gas that had been pushed down from the top of the tube by launch-induced fluid motion and that the smaller bubbles were generated by the other two mechanisms.

Figures 5 and 6 show that during the course of the experiment the smaller bubbles disappeared and the large bubbles remained stationary. The bubbles at the interface grew larger and were incorporated into the growing crystal as the experiment proceeded. These observations are much more apparent in the motion picture. Figures 7, 8, and 9 are photographs of montages which were made by cutting 8 x 10 in. prints of selected frames and pasting them together. They show the sequence of events more clearly than individual still photos. Figure 10 is a similar montage from a ground base simulation. These figures show that there was little, if any, motion of those bubbles which did not contact with the interface. They also show that nucleation and growth of bubbles occurs at the advancing interface in each of the three flight specimens and that these bubbles are some-times displaced.
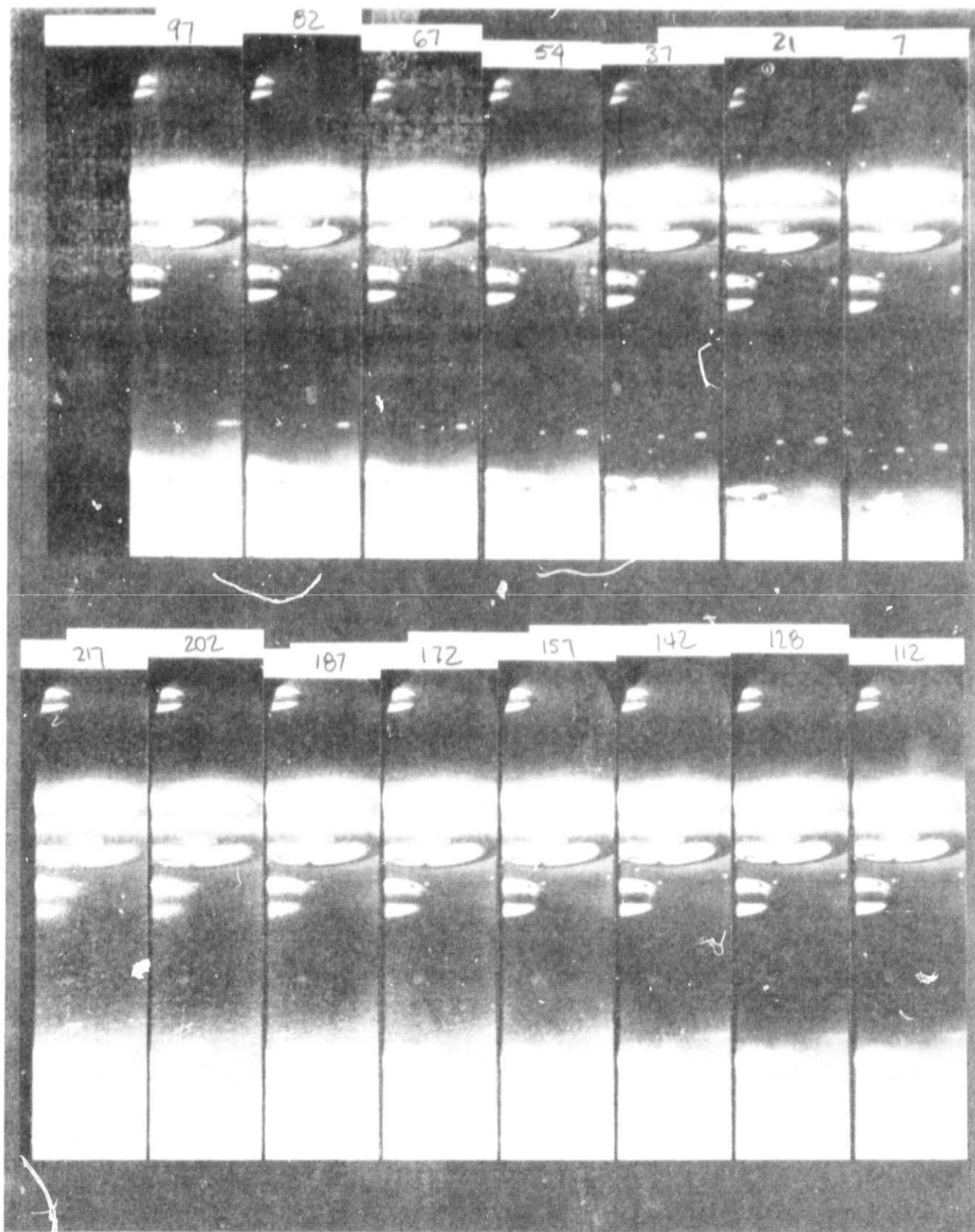
Figure 7 Composite photograph of specimen B. The frame sequence number, n, is above each view; the time since lift off is n+80s

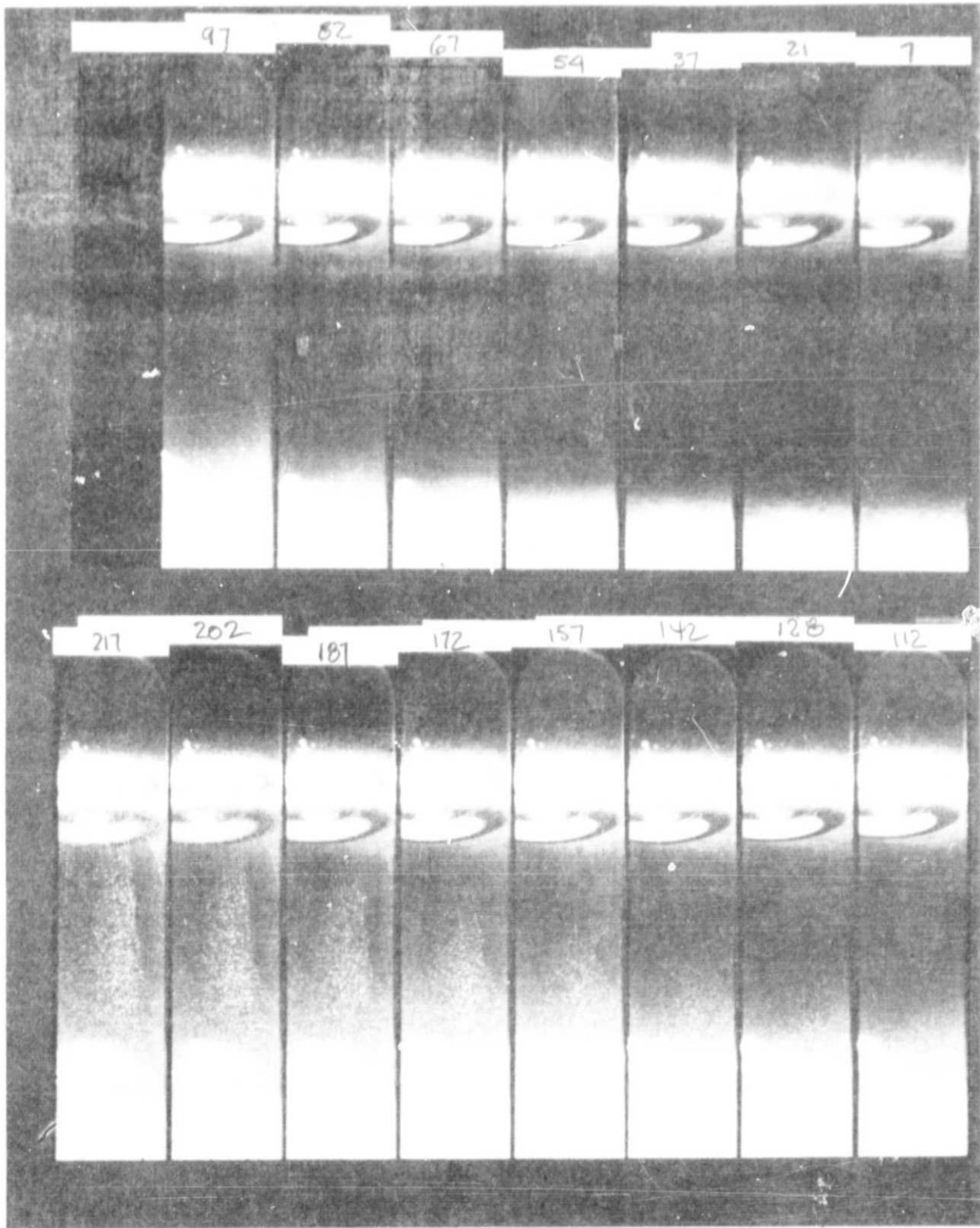12

Figure 8 Composite photograph os specimen C, same conditions as Fig. 7
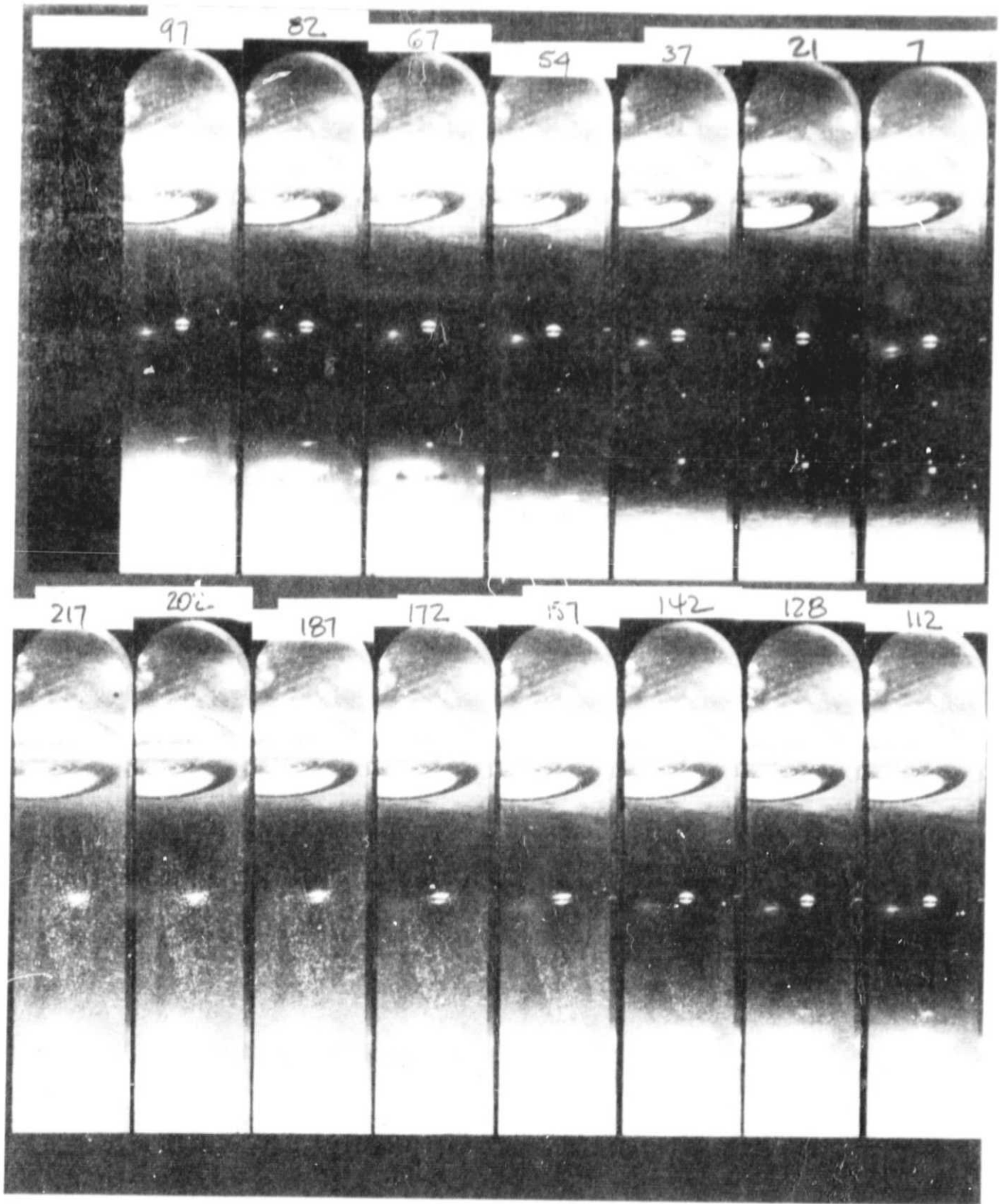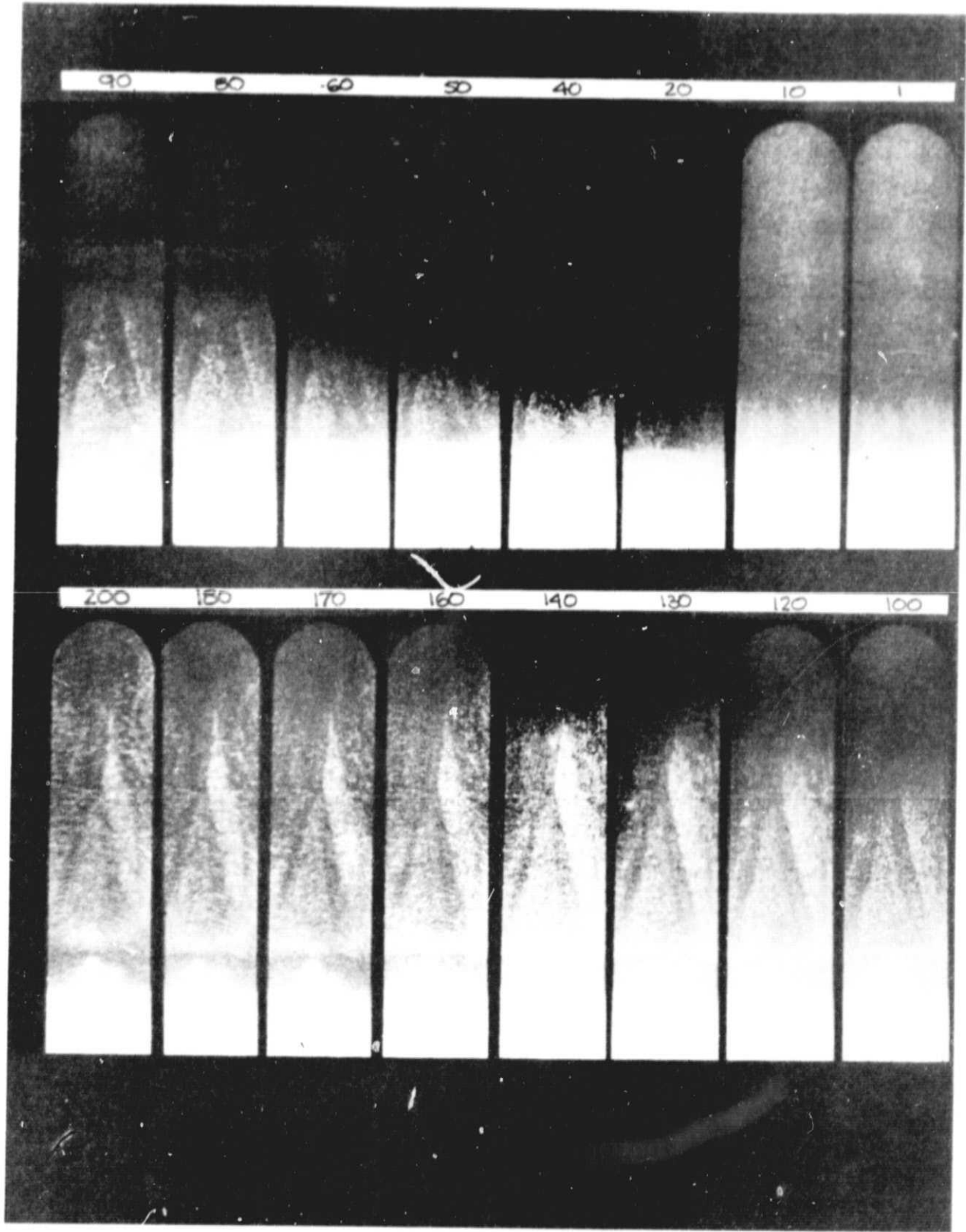
Figure 9 Composite photograph of specimen D, same conditions as Fig. 7

14

Figure 10 Composite photograph of a specimen from a ground base simulation

15

The motion of bubbles at the interface was sometimes abrupt, as is obvious in the motion picture. An example is shown in Fig. 11 which shows two sequential views of specimen D. The two views were taken one second apart, and the bubble moved 0.8mm in that time. It was stationary for many frames before and after. The ground based simulation specimen produced almost no incorporation of bubbles at the interface. Numerous bubbles were generated at the interface but they were eventually detached and rose rapidly under the influence of normal buoyancy forces.

Numerous small bubbles disappeared in the first 30 to 50 seconds, particularly in specimens D and B. The origin of this phenomenon is unclear. In general, the solubility of a gas in organic liquids increases as the temperature decreases. Thus, the small bubbles could have merely been dissolving into the melt as it cooled. However, data on the solubility of A, H_2, and N_2 in CCl_4 shows mixed behavior and in some cases the gas solubility decreases with decreasing temperature. We do not know how the solubility behaves in CBr_4, and ground based experiments are planned to determine this. Other possibilities include Ostwald ripening or simply that the bubbles were transported during launch into a region of melt not saturated with gas.

Figure 11 A sequence of two views of specimen D taken one second apart

16

Figures 7, 8, 9 and 10 allow us to estimate growth rate of the crystals. It is sometimes difficult to decide exactly where the crystals ended and the liquid began. This is not unusual since the material was not extremely pure and an extensive dendritic mushy zone was expected and found. Also, the lighting system was designed for bubble observations and was not optimum for observing the interface. However, we can subjectively define three "interfaces", namely, the fastest dendrite tip, a transparent interface, and a translucent interface. Measurements of the positions of these interfaces from specimen B are shown in Fig. 12. The average growth rates of these three "interfaces" are 110, 10, and 4 μm/s, respectively. Measurements on the two other flight specimens gave similar values. Similar data for a ground base simulation specimen gave values of 2.5 and 120 μm/s for the transparent and fastest dendrite interfaces. We see that although the block cooled significantly more slowly in flight than during the GBS, the crystals grew at much the same rate. This was due to poor heat transfer between the glass specimen tube and the aluminum block in a vacuum.

C. Structural Observations

The flight specimens contained large grown-in voids (gas bubbles). These are illustrated in the X-radiographs shown in Fig. 13*. All three of the flight specimens contained voids in the portion of the crystal which was grown during the microgravity interval. The GBS crystals did not contain voids. Figure 14 is a macrograph of flight specimen D in which part of a subsurface void is visible. The circumference of the crystal was complete in all cases, i.e., the voids were confined to the center of the crystal and did not intersect the external surface. Figure 15 is a macrograph of a portion of the melt-back interface and shows that a separation had occurred at the interface. Since the details on either side of the interface were almost exact replicas of each other, it is concluded that this separation occurred after solidification, perhaps during the shock of reentry or landing. It is also possible that the separation occurred because of thermal contraction, although this did not occur in the GBS samples. Thermal contraction is likely to be the cause of the observed separation at many of the grain boundaries in both flight and GBS specimens. It is interesting to note that the surfaces of the CBr_4 grain boundaries revealed in this manner show a very rounded or pebbly topography (due to the dendritic solidification). This is in contrast to the more angular topography generally observed in embrittled metallic grain boundaries and is possibly due to smoothing after separation. The smoothing may have been due to a high evaporation rate. It is also possible that the boundaries are rounded in the as grown conditions.

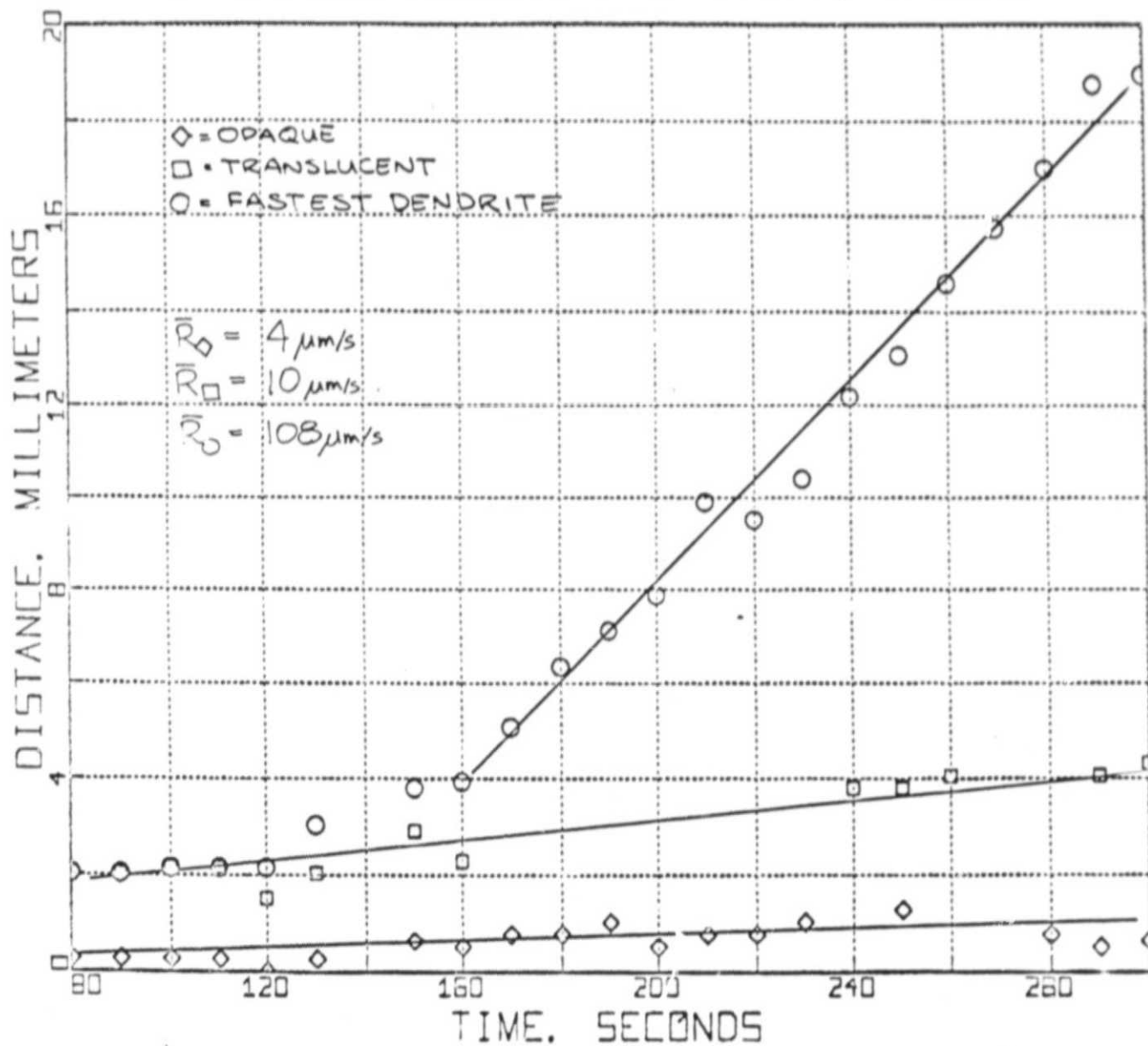* The size of the voids is exaggerated by the X-ray technique.

17

Figure 12 Interface position as a function of time, specimen B, flight

18
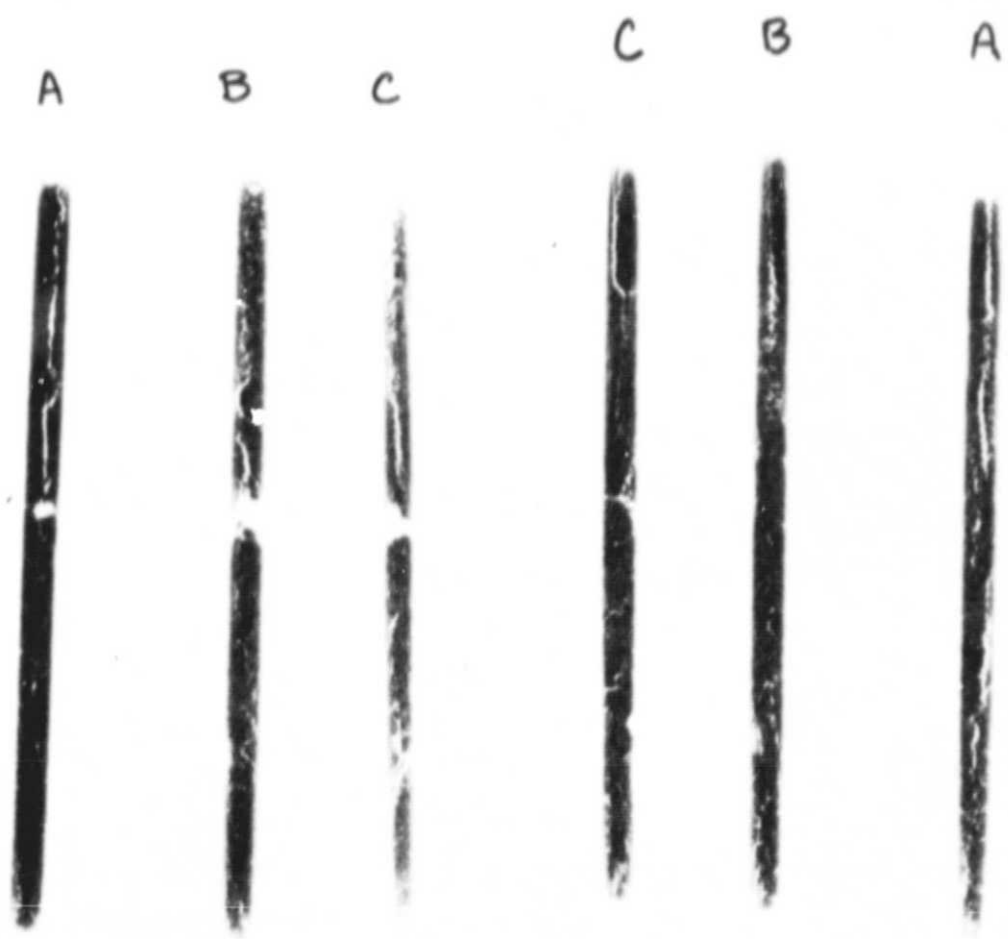
Figure 13 X-radiographs of the three flight specimens, on the left, and three GBS specimens, on the right

Figure 16 shows several grains in a CBr_4 specimen. The misorientation across the grain boundary can be readily seen from the dendritic pattern in each crystal. The pattern was probably caused by segregation of impurities to the regions between dendrite arms. Using this observation as a guide, the grain size of the specimens was estimated by simply counting the number of linear defects visible around the circumference of the crystal at the interface. The results are shown in the following Table. Note that the flight specimens were slightly finer grained than the GBS specimens.

19

Grain Size (mm) of Three Different Type Specimens.

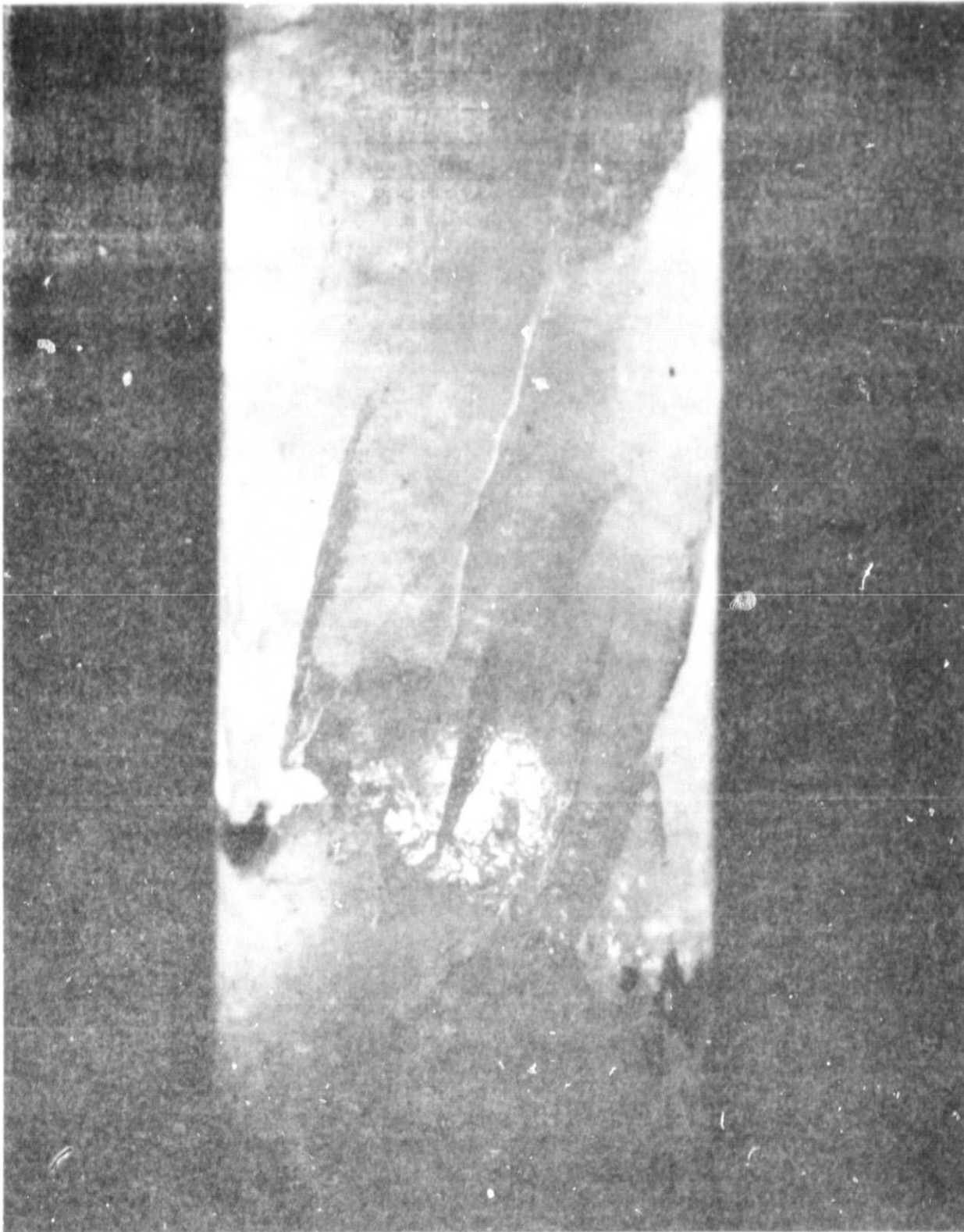|	A	H_2	N_2
Flight	2.3	2.1	1.9
GBS 18 Aug 75	2.8	2.5	2.8
GBS 21 Aug 75	2.5	3.6	3.1
GBS 4 Sep 75	4.2	3.6	3.1

Figure 14 Macrograph of specimen D, flight. The melt back interface is roughly horizontal and located toward the bottom of the picture. The growth direction is upward. The total width of the specimen was 10mm.

21

Figure 15 Macrograph of specimen C, flight. Same conditions as Fig. 14

Figure 16 Macrograph of specimen D, flight. Same conditions as Fig. 14

23

IV. DISCUSSION

The results of this experiment show for the first time, generation, coalescence, and incorporation of bubbles at a solidification interface in the absence of buoyancy forces. The observations are not yet quantitative nor do they form part of a coherent scientific description of the process of bubble interface interaction. These tasks will be pursued on later flights. The motion picture record of the experiment adds an extra dimension of insight into the dynamics of the process. In addition, we have gained understanding of the sounding rocket environment.

The seemingly incredible juxtaposition of 70 seconds of rapid spin, violent acceleration and thrust, followed by 300 seconds in which all imposed accelerations are less than 10^{-4}g, does not appear to preclude meaningful experiments. Fluid motion seems to have been significant during the launch phase as evidenced by the particle decorated vortex in sample A and the distribution of bubbles in samples B and D. The sample tube was aligned with the axis of the rocket and approximately 100mm off center. Each tube had an inside diameter of 8mm and was launched with the hot end up. From the shape of the vortex and location of the bubbles, particularly the large bubbles, we conclude that the circumferential fluid velocity (i.e., in the plane normal to the rocket axis) was significantly greater than the axial velocity (along the axis of the rocket). Thus, there was significant interface erosion or melt back, but the fluid motion was not vigorous enough to completely level the temperature gradient or distribute the foreign bodies throughout the liquid. Some leveling of the temperature gradient did occur as is seen in Fig. 3. It is not yet established how much of a thermal lag is present between the aluminum block and the specimen fluid but the data in Fig. 3 must underestimate the leveling effect. Nevertheless it is thought that a substantial temperature gradient remained in the liquid at the beginning of the microgravity interval. The damping of fluid motion was extremely rapid. De-spin occurred at approximately 64s and the rate control system was activated immediately afterward; microgravity conditions were established by 75s. Our first photograph at 80s showed no evidence of fluid motion; this macroscopically quiescent state persisted to the end of the experiment at approximately 300s. This is a highly favorable result and removes a major uncertainty in plans for future experimentation.

The immobility of bubbles in a temperature gradient is the most surprising observation of this experiment. The only previous work in this field (Ref. 4) leads to the prediction that bubbles should move with a velocity, v, given by

$$v = \frac{d\gamma}{dT} \cdot \frac{dT}{dz} \cdot \frac{r}{3\mu} \tag{1}$$

or

$$Re = \frac{M}{3} \tag{2}$$

where $d\gamma/dT$ is the temperature dependence of the surface tension, dT/dz the imposed temperature gradient, r the bubble radius, μ the fluid viscosity, Re the reynolds number and M the Marangoini number. For a 1mm bubble with $d\gamma/dT = -0.1$ dyn/cm°C, $d\gamma/dT = -0.1$ dyn/cm°C, $dT/dZ = 5°C/cm$ and $\mu = 2$ cp this formula gives an expected velocity of about 4 mm/s. This prediction is not borne out in our experiment. Crude measurements of the bubble motion give an upper limit to the observed velocity of approximately 10^{-2} mm/s. Equation 1 is the result of simplifying assumptions, but should nevertheless give the correct order of magnitude for bubble velocity.

We can generate at least four hypotheses to explain the discrepancy as follows:

a) $d\gamma/dT = 0$. If the surface tension of CBr_4 does not vary with temperature in the region of interest then there would be no driving force for bubble migration. We have measured $d\gamma/dT$ for our CBr_4 in the laboratory under conditions which should approximate those of the flight experiment. The results are shown in Fig. 17 and give us $d\gamma/dT = -0.11$ dyn/cm'C, a fairly typical value for organic liquids.

Thus, we discount this hypothesis.

b) $dT/dZ = 0$. If no temperature gradient were present, there would be no driving force for migration. A stable temperature gradient certainly existed before launch, but perhaps this was almost completely eliminated by launch-induced fluid motion. As discussed above, fluid motion did occur. The imposed accelerations were primarily downward, due to lift off, and radial, due to spin and de-spin. The longitudinal forces would not tend to cause much mixing since the denser (cooler) fluid was at the bottom. Transient spin can be very effective at mixing but in this case it did not seem to have been as evidenced by the position of the particles in specimen A. Further evidence that the temperature gradient was not eliminated is provided by the observation that the freezing rate was not much different in
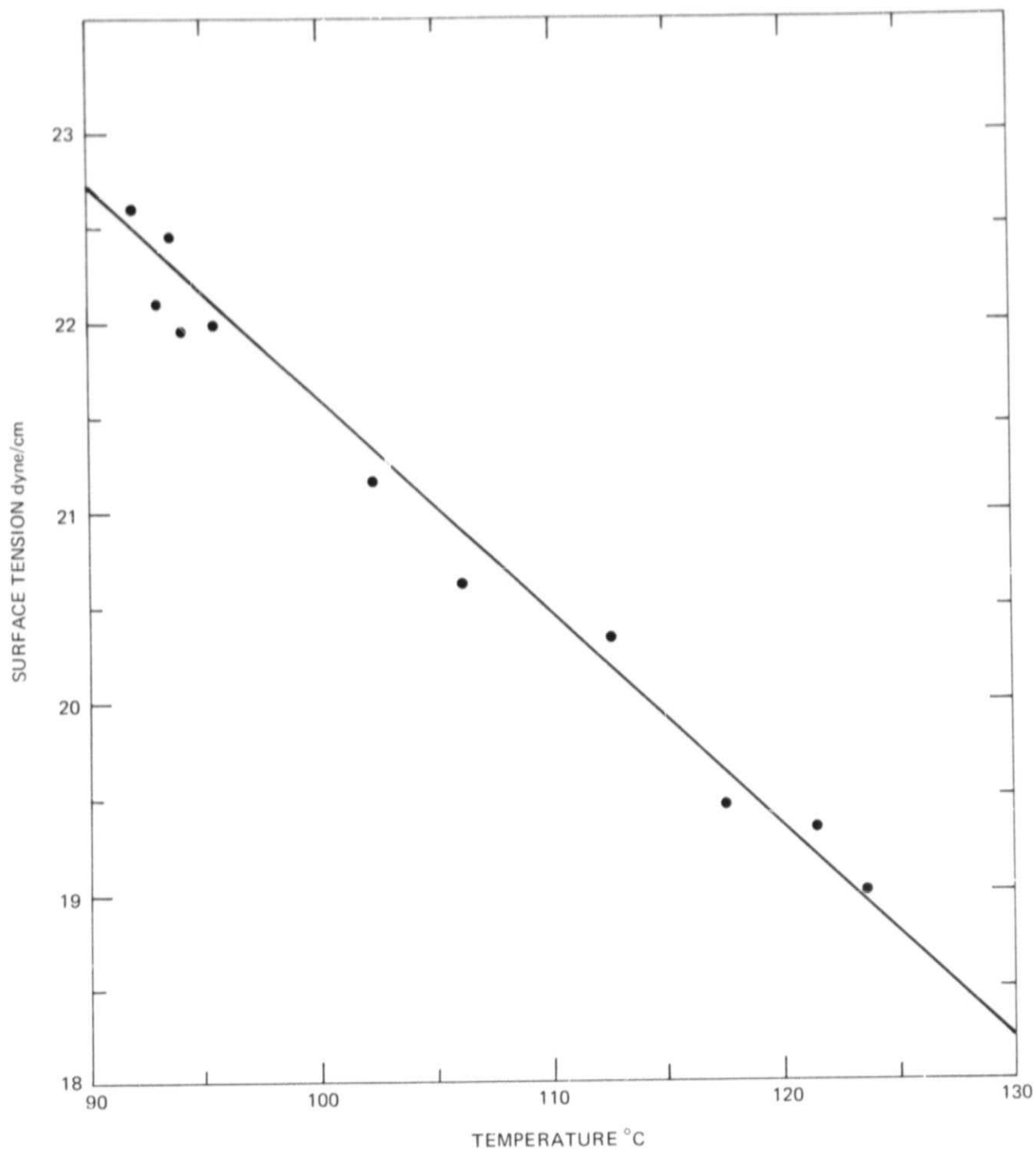
25

Figure 17 Surface tension of CBr$_4$ as a function of temperature

26

the flight and GBS tests. If the temperature gradient had been much lower, then we would have observed more rapid crystal growth.

c) Pinning. If the bubbles were pinned by being in contact with the tube wall or solid material, then they would not be free to migrate. It is thought that most of the bubbles were not in contact with solid CBr_4, at least at the beginning of the experiment, because we see no indication of solid being present in the liquid near the bubbles. It is possible that all of the bubbles were touching the tube wall; it is very difficult to evaluate this from the photographs. It is improbable, however, that all of the bubbles would be against the wall, unless the fluid or heat flow had been such as to cause this. However, a hotter wall might have causes migration of the bubbles toward the wall and thus trapped them. Since the aluminum block cooled faster than the specimen tube, it is thought unlikely that the tube wall was hotter than the CBr_4. The fluid flow pattern may have thrown all of the bubbles to the wall, but it is impossible to evaluate the likelihood of this occurrence.

d) Impurity Segregation. It is possible that impurities could have segregated to the surface and arrested bubble motion. We distinguish between two cases: (1) the lack of an energetic driving force due to equilibrium segregation, and (2) a kinetic limitation on the rate of matter transport. Equilibrium segregation, as defined in Ref. 6, is limited to coverages on the order of a monolayer (Ref. 7) and is strongly temperature dependent. This strong temperature dependence of adsorption can lead to a $d\gamma/dT = 0$ or even $d\gamma/dT < 0$ (Refs. 8 & 9). This would naturally cause the bubble to be static or to migrate in the opposite direction. We do not believe this to have been the case in this experiment because our laboratory measurements of $d\gamma/dT$ would have shown this effect as mentioned in IV(a).

A kinetic limitation might have arisen if a strongly segregating impurity was present, was concentrated to monolayer or greater thickness in the surface, and the rate of transport of an impurity molecule across the interface between the segregated layer and the bulk liquid was slow. This situation has been observed in bubble buoyancy experiments and might account for greatly reduced migration rates even though a negative $d\gamma/dT$ still existed. No extensive or obvious surface layer was observed in the photographs, in microscopic observations of GBS tests, or during the laboratory measurements of $d\gamma/dT$. However, this does not preclude its existence.

27

V. SUMMARY

The effect of gravity on the grown-in void content in our CBr_4 specimens strikingly illustrates the potential problem posed by bubble generation during solidification in the orbital environment. These results demonstrate the reality of the problem and confirm the viability of our experimental approach. We have observed that during terrestrial solidification bubbles nucleate and grow at the interface, but generally detach and float to the surface of the melt. Thus, we usually obtain a specimen which is free of large voids. However, in free fall, bubble nucleation and growth also occur, but the bubbles do not detach from the interface and the dendritic gorwth front is able to go around the bubbles, this forming a void.

Coalescence of bubbles trapped in the mushy zone was observed to occur in an abrupt manner, similar to the collapse of soap films. The grain size of the low-gravity specimens was finer than that of the GBS specimens. Bubbles, 50μm to 4mm in diameter, situated in the melt well ahead of the interface did not migrate to the hot end of the sample tube; this is contrary to the predictions of thermal migration of bubbles in the absence of gravity. Several possible explanations for this behavior are given.

VI. REFERENCES

1) Jackson, K. A., Hunt, J. D., Umlman, D. R., and Seward, T. P.,
   TRANS. TMS-AIME 236, 149 (1966).

2) Hodgman, C. D., ed. Handbook of Chemistry and Physics, 39th edition Chemical
   Rubber Publishing Co. (1958).

3) Papazian, J. M. and Wilcox, W. R., "Thermal Migration of Bubbles and Their
   Interaction with Solidification Interfaces," Research Proposal file no. 74-127 NAS,
   February 1975.

4) Young, N. O., Goldstein, J. S., and Block, M. J., J. Fluid Mech., 6, p. 350 (1959).

5) Grodzka, P. G., Proceedings of the Third Space Processing Symposium Skylab Results,
   NASA G. C. Marshal Space Flight Center p. 691 (1974).

6) McLean, D., Grain Boundaries in Metals, p. 116, Oxford Univ. Press (1957).

7) Cahn, J. W., Hilliard, J. E., Acta Met. 7, p. 219 (1959).

8) Jones, H., and Leak, G. M., Metal Science Journal 1, p. 211 (1967).

9) Jones, H., and Leak, G. M., Acta Met. 14, p. 21 (1966).